



International Congress of Science and Technology of Metallurgy and Materials, SAM –  
CONAMET 2014

## Combustion synthesis of ultrafine powders of $\text{Co}_3\text{O}_4$ for selective surfaces of solar collectors

M. Celeste Gardey Merino<sup>a,\*</sup>, M. Emilia Fernández de Rapp<sup>b</sup>, Mónica Pinto<sup>c</sup>, M. Elisa Etchechoury<sup>c</sup>, M. Silvina Lassa<sup>d</sup>, J. Miguel Martín Martínez<sup>e</sup>, Gustavo E. Lascalea<sup>f</sup>, Patricia G. Vázquez<sup>g</sup>

<sup>a</sup>Grupo CLIOPE, Universidad Tecnológica Nacional - Facultad Regional Mendoza, Rodríguez 273, Mendoza (M5502AJE), Argentina

<sup>b</sup>CINSO-CITEDEF-CONICET, J.B. de La Salle 4397, Villa Martelli, Buenos Aires (B1603ALO), Argentina

<sup>c</sup>INTI, Av. Gral. Paz 5445 (B1650KNA), Buenos Aires, Argentina

<sup>d</sup>MEByM-IANIGLA-CONICET-Mendoza, Av. Ruiz Leal s/n Parque Gral. San Martín, CC. 131, M5502IRA, Mendoza, Argentina

<sup>e</sup>Laboratorio de Adhesión y Adhesivos de la Universidad de Alicante, Ctra. San Vicente s/n (03080), Alicante, España

<sup>f</sup>LQA-IANIGLA-CONICET-Mendoza, Av. Ruiz Leal s/n Parque Gral. San Martín, CC. 131, M5502IRA, Mendoza, Argentina

<sup>g</sup>CINDECA-CCT-CONICET - La Plata, Universidad Nacional de La Plata, Calle 47 N° 257, La Plata (B1900AJK), Buenos Aires, Argentina

### Abstract

Solar selective paints, with the addition of  $\text{Co}_3\text{O}_4$  as a pigment, are used to improve energetic efficiency in solar collectors. Although  $\text{Co}_3\text{O}_4$  has been obtained by different methods, references about combustion synthesis are scarce.  $\text{Co}_3\text{O}_4$  powders have been synthesized by stoichiometric and non-stoichiometric routes using aspartic acid (Asp) or tri-hydroxi-methyl-aminomethane (Tris) as fuels. The samples were calcined in air at 500 °C. They were characterized by X-ray diffraction, scanning electron microscopy, transmission electron microscopy, thermogravimetric analysis, differential scanning calorimetry, Fourier transform infrared spectrum and the specific surface area of the samples was determined by means of the Brunauer–Emmett–Teller technique. The optical properties of pigments were assessed by means of a spectrophotometer. In all cases, powders exhibited the crystalline structure of  $\text{Co}_3\text{O}_4$ . A minimum crystallite average size of 29 nm was observed for powders obtained by the “stoichiometric/Asp” combustion route, while a maximum value of 41 nm was stated for powders obtained by the “non-stoichiometric/Asp” combustion process. The average particle size ranged between 50 and 100 nm. The powders obtained by the “stoichiometric/Asp” method were selected to study their optical properties; their solar absorption value was 86%. Solar selective surfaces composed by  $\text{Co}_3\text{O}_4$  pigments and an alkyd resin were obtained and applied over copper or aluminum substrates. In both

\* Corresponding author. Tel.: +542615244694; fax: +542615244531.

E-mail address: [mccgardey@frm.utn.edu.ar](mailto:mccgardey@frm.utn.edu.ar)

cases, solar absorptance was of 93% and comparable with similar solar selective surfaces, but the thermal emittance value was higher than 90%, as a consequence of the large width of the films.

© 2015 The Authors. Published by Elsevier Ltd. This is an open access article under the CC BY-NC-ND license (<http://creativecommons.org/licenses/by-nc-nd/4.0/>).

Peer-review under responsibility of the Scientific Committee of SAM-CONAMET 2014

*Keywords:* Cobalt oxide nanoparticles; gel combustion-process; solar absorptance; optical spectroscopy; X-ray diffraction

## 1. Introduction

In this work, the results of the research about materials used for solar heating of water in thermal collectors are presented. Solar selective surfaces are used to improve energetic efficiency of solar collectors when they fulfill two requirements: high absorptance within the solar radiation wavelength range (0.3–3  $\mu\text{m}$ ) and a low emittance across the thermal wavelength domain (above 3  $\mu\text{m}$ ). Paint coatings are also an important class among selective surfaces (Trease et al. (2013)). In particular the  $\text{Co}_3\text{O}_4$ , a metal oxide pigment, is used in these paints due to its high absorption in the solar spectrum. This paint usually covers aluminum that presents low emittance in the thermal wavelengths (Van Buskirk (1982)). This high absorption in the solar spectrum can be explained by the numerous, electronic transitions allowed between the *d*-orbitals of Co ions, not fully occupied with electrons, alike others oxides of transition metals (Mn, Fe, Cr) (Vince et al. (2003)).  $\text{Co}_3\text{O}_4$  is obtained by different methods, such as: precipitation (Pal et al. (2010)), sol-gel (Luisetto et al. (2008)), spray-pyrolysis (Avila et al. (2004)) and hydrothermal synthesis (Gui et al. (2004)). Other methods like reflux (Ozkaya et al. (2009)), mechanochemical (Yang et al. (2004)), ultrasound assisted techniques (Askarinejad et al. (2009)), on biotemplates (Yang et al. (2004)) and chemical vapor deposition (CVD) (Barreca et al. (2011)) using organic complexes (Thangavelu et al. (2011)) and by gel-combustion synthesis (Venkateswara et al. (2008); Toniolo et al. (2010)) are suitable as well.

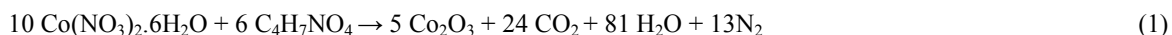
In this work, two new gel-combustion routes for the synthesis of  $\text{Co}_3\text{O}_4$  nanopowders with aspartic acid (Asp) or tri-hydroxi-methyl-aminomethane (Tris) as fuels are presented. The first route is a conventional stoichiometric process while the second one is a non-stoichiometric pH-controlled process. The resulting powders were calcined in air at 500 °C. Once calcined, the samples were characterized by X-ray diffraction (XRD), scanning electron microscopy (SEM), transmission electron microscopy (TEM), Fourier transform infrared spectrum (FTIR), thermogravimetric analysis (TGA) and differential scanning calorimetry (DSC). Optical properties of these pigments were assessed with a spectrophotometer. With the so-obtained, stabilized  $\text{Co}_3\text{O}_4$  powders a solar selective surface was made and characterized by spectrophotometry.

## 2. Experimental procedure

### 2.1. Synthesis of $\text{Co}_3\text{O}_4$ nanostructured powders

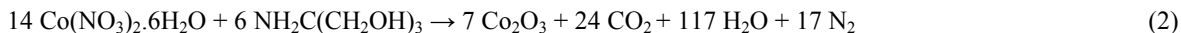
$\text{Co}_3\text{O}_4$  nanopowders were obtained by gel-combustion processes using either Asp ( $\text{C}_4\text{H}_7\text{NO}_4$ ) or Tris ( $\text{C}_4\text{H}_{11}\text{NO}_3$ ) as fuels. The first one is a conventional, stoichiometric process, while the second is a non-stoichiometric, pH-controlled process. These chemical routes were performed using reagents of analytical grade. The final calcinations were at 500 °C during 2 h.

The stoichiometric process was performed as follows: 5 g of  $\text{Co}(\text{NO}_3)_2 \cdot 6\text{H}_2\text{O}$  (Aldrich) and 1.37 g of Asp ( $\text{C}_4\text{H}_7\text{NO}_4$ , Aldrich) were dissolved in distilled water to obtain a homogeneous solution, with a pH=3. The Asp/Co molar ratio chosen was 6/10 (0.6) as calculated on the basis of the following stoichiometric reaction of combustion:



This precursor solution was concentrated on a hot plate at 250°C until obtaining a viscous gel. Soon after, it ignited and the combustion process evolved without flame. These powders were labeled  $\text{Co}_3\text{O}_4$ -S-Asp.

For the stoichiometric nitrate–Tris route the same procedure was applied starting from the same mass of 5 g of  $\text{Co}(\text{NO}_3)_2 \cdot 6\text{H}_2\text{O}$  but, in this case, the stoichiometric reaction required a Tris/Co molar ratio of 6/14 (0.43) based on the following stoichiometric reaction of combustion



These powders were labeled  $\text{Co}_3\text{O}_4\text{-S-Tris}$ .

For the non-stoichiometric pH-controlled nitrate–Asp route a first solution was prepared from 5 g of  $\text{Co}(\text{NO}_3)_2 \cdot 6\text{H}_2\text{O}$  (Aldrich), 10ml of  $\text{HNO}_3$  (concentrated) and an amount of sufficient distilled water to reach a volume of 100mL. This solution was concentrated in a hot plate to reduce the amount of nitrates, and then distilled water was added again to obtain 100 mL of solution. A second solution was prepared by dissolving 6.86 g of Asp in distilled water. Then, both solutions were carefully mixed resulting in a homogeneous mixture with an Asp/Co molar ratio of 3. This ratio was chosen based on the “oxidative valence criterion”, taking into account previous studies of similar processes where the optimum ratio for a pH controlled nitrate–glycine route to synthesize  $\text{ZrO}_2\text{-CeO}_2$  solid solutions was found to be 5 (Lascalea (2004)). Then,  $\text{NH}_4\text{OH}$  (diluted 1:1, Merck) was added to obtain a precursor solution with pH=7. This solution was then concentrated on a hot plate at 250 °C until it turned into a viscous gel, which finally burned with flames due to the expected exothermic reaction of combustion. These powders were labeled  $\text{Co}_3\text{O}_4\text{-NS-Asp}$ .

For the non-stoichiometric pH-controlled nitrate–Tris route the same procedure was used, starting from the same mass of 5 g of  $\text{Co}(\text{NO}_3)_2 \cdot 6\text{H}_2\text{O}$  but, also based on the above-mentioned criterion, the Tris/Co molar ratio was 2.12 and the pH obtained for the precursor solution resulted was 8. These powders were labeled  $\text{Co}_3\text{O}_4\text{-NS-Tris}$ .

## 2.2. Preparation of selective surfaces

The paint was prepared with a base of an alkyd resin and the obtained  $\text{Co}_3\text{O}_4\text{-S-Asp}$  powders used as pigments. Then, aluminum and copper metallic substrates were properly cleaned and degreased. The paint was applied on metallic substrates with a brush and cured at 25 °C and 60% of moisture. Two solar selective surfaces were obtained.

## 2.3. Materials characterization

The phases present in as-synthesized  $\text{Co}_3\text{O}_4$  nanopowders were identified by XRD using a Philips PW 3710 diffractometer with Cu-K $\alpha$  radiation. Our data were compared with those reported in the Inorganic Crystal Structure Database (ICSD). The average crystallite size was determined from the broadening of Bragg peaks using the Scherrer equation. The powders morphology was analyzed by SEM (Philips 505 microscope) and TEM (JEOL 100 CX II microscope). The operation voltage was 100 kV. In both cases, the preparation of specimens was performed following conventional procedures. FTIR of powders were obtained in a Bruker IFS 66 equipment. TGA was carried out with a detector SHIMADZU TGA-51 at a rate of 20 °C/min, between environmental temperature and 600 °C, in air with a platinum cell. DSC measurements were carried out with a detector SHIMADZU DSC-50 at a rate of 20 °C/min, between environmental temperature and 600 °C in air, with an aluminum cell. The optical characteristics, transmission and reflection of samples in the solar spectrum, were studied with a spectrophotometer of double beam SHIMADZU, UV-3101PC with an integrating sphere model 3100. From the above measurements the solar absorptance ( $\alpha_s$ ) was calculated. The studied pigments were placed in a basin of quartz.

The solar absorptance values of samples were determined in the solar spectrum ( $0.3 \mu\text{m} < \lambda < 3 \mu\text{m}$ ) with the above-described spectrophotometer, using normal/hemispheric geometry with a specular component included. From the obtained values, the spectral characteristics were calculated as follows:

Solar transmittance ( $\tau_s$ ):

$$\tau_s = \frac{\sum_{\lambda=300\text{ nm}}^{2500\text{ nm}} \tau_\lambda \times S_\lambda \times \Delta\lambda}{\sum_{\lambda=300\text{ nm}}^{2500\text{ nm}} S_\lambda \times \Delta\lambda}, \quad (3)$$

where  $\tau_\lambda$  is the spectral transmittance of the surface between 300 nm and 2500 nm;  $S_\lambda$  is the relative normalized spectral distribution of global radiation for air mass = 1.5 and  $\Delta\lambda$  is the range of consecutive wavelength. In this case  $\Delta\lambda$  was equal to 5 nm between 300 nm and 400 nm, 10 nm between 400 nm and 800 nm, and 50 nm between 800 nm and 2500 nm.

Solar reflectance ( $\rho_s$ ):

$$\rho_s = \frac{\sum_{\lambda=300\text{ nm}}^{2500\text{ nm}} \rho_\lambda \times S_\lambda \times \Delta\lambda}{\sum_{\lambda=300\text{ nm}}^{2500\text{ nm}} S_\lambda \times \Delta\lambda}, \quad (4)$$

where  $\rho_\lambda$  is spectral reflectance of the sample between 300 nm and 2500 nm. The solar absorptance ( $\alpha_s$ ) is the result of the following expression

$$\alpha_s = 1 - \rho_s - \tau_s. \quad (5)$$

Thermal emittance measurements were carried out at environmental temperature with a “Devices and Service AE” portable emisometer.

Finally, their width was measured with a caliper.

### 3. Results and discussion

According to XRD patterns shown in Fig. 1, the spinel crystal structure of  $\text{Co}_3\text{O}_4$  corresponding to database ICSD N° 36256 was observed in all produced powders.

The average crystallite sizes calculated by Scherrer equation are reported in Table 1. This table shows a minimum crystallite average size of 29 nm for “stoichiometric/Asp” powders while a maximum value of 41 nm was stated for “non-stoichiometric/Asp” powders. In brief, powders obtained by stoichiometric routes have a lower average crystallite size than those obtained by non-stoichiometric processes. Similar tendencies are observed in  $\text{Co}_3\text{O}_4$  powders synthesized by combustion using glycine and urea as fuels (Toniolo et al. (2010)).

Specific surface areas obtained from  $\text{Co}_3\text{O}_4$  powders are present in Table 1, the higher value corresponding to  $\text{Co}_3\text{O}_4$ -S-Asp powders. Additionally, the specific surface areas of powders obtained using stoichiometric routes are higher than those observed from powders obtained by non-stoichiometric routes, for the same fuel.

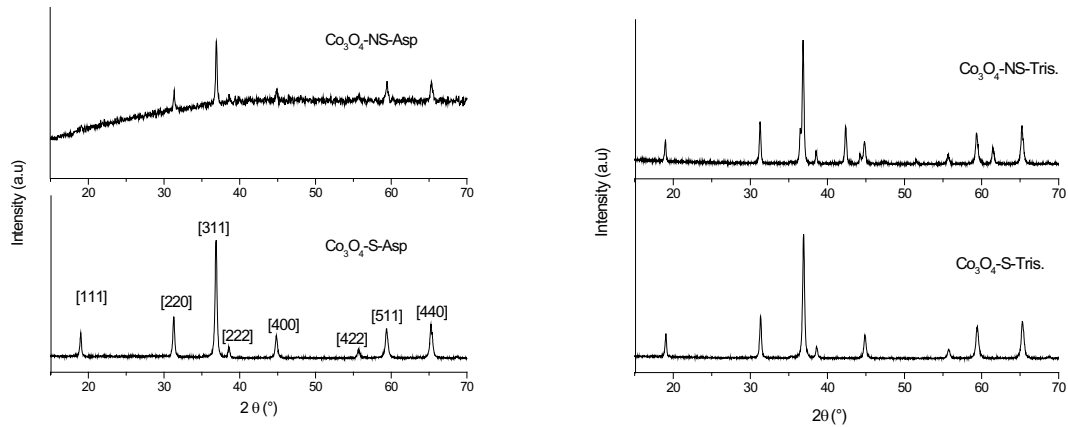


Fig. 1. XRD patterns of obtained samples.

Table 1. Average crystallite sizes and Brunauer-Emmett-Teller (BET) specific surface areas obtained for  $\text{Co}_3\text{O}_4$  powders.

Powder	BET specific surface area ( $\text{m}^2/\text{g}$ )	Crystallite size (nm)
$\text{Co}_3\text{O}_4\text{-S-Asp}$	20	29
$\text{Co}_3\text{O}_4\text{-NS-Asp}$	4	41
$\text{Co}_3\text{O}_4\text{-S-Tris}$	14	33
$\text{Co}_3\text{O}_4\text{-NS-Tris}$	9	33

By SEM measurements, it was observed that all samples exhibited a high degree of agglomeration, as displayed in Figs. 2(a)-(d). In particular more compact structures are observed in powders resulting from non-stoichiometric routes. A similar agglomeration is evidenced in  $\text{Co}_3\text{O}_4$  powders synthesized by combustion using glycine and urea as fuels (Venkateswara et al. (2008)). In Figs. 2(e) and (f) micrographs with a higher resolution are shown for  $\text{Co}_3\text{O}_4\text{-NS-Asp}$  and  $\text{Co}_3\text{O}_4\text{-NS-Tris}$ , respectively. Thanks to the optimal resolution one can easily observe polyhedral particles in the second case.

As estimated through TEM observations the particle size ranges from 50 to 100 nm, (scale line = 20 nm), as shown in TEM micrographs of Fig. 3 for all obtained powders. The polyhedral shape of particles is also evidenced, but an octahedral shape is more frequently observed as in the case of  $\text{Co}_3\text{O}_4$  particles obtained by precipitation methods too (Tang et al. (2008)).

DSC and TGA graphics corresponding to  $\text{Co}_3\text{O}_4\text{-NS-Asp}$  are shown in Fig. 4. At 400 °C an exothermic transformation with a release of energy of about 5 mW was observed. Additionally, a 0.15 mg loss of weight was evidenced at the same temperature. Both changes could be related to a transition from CoO to  $\text{Co}_3\text{O}_4$  according to the phases found by Toniolo et al. (2010), like Co, CoO and  $\text{Co}_3\text{O}_4$ , in ashes collected after combustion synthesis of cobalt oxides.

The IR spectra evidenced two distinct and sharp bands at 622 ( $\nu_1$ ) and 727 ( $\nu_2$ )  $\text{cm}^{-1}$  stemming from stretching vibration modes of the metal–oxygen bond. These bands confirm the presence of  $\text{Co}_3\text{O}_4$  spinel oxide, since the  $\nu_1$  band characterizes  $\text{Co}^{3+}$  vibration in octahedral sites of the spinel and  $\nu_2$  band characterizes  $\text{Co}^{2+}$  vibration in tetrahedral ones (Gui et al. (2004)). Similar bands corresponding to  $\nu_1$  y  $\nu_2$  are observed in cobalt oxides synthesized by microwave methods (Al-Tuwirqi et al. (2011)).

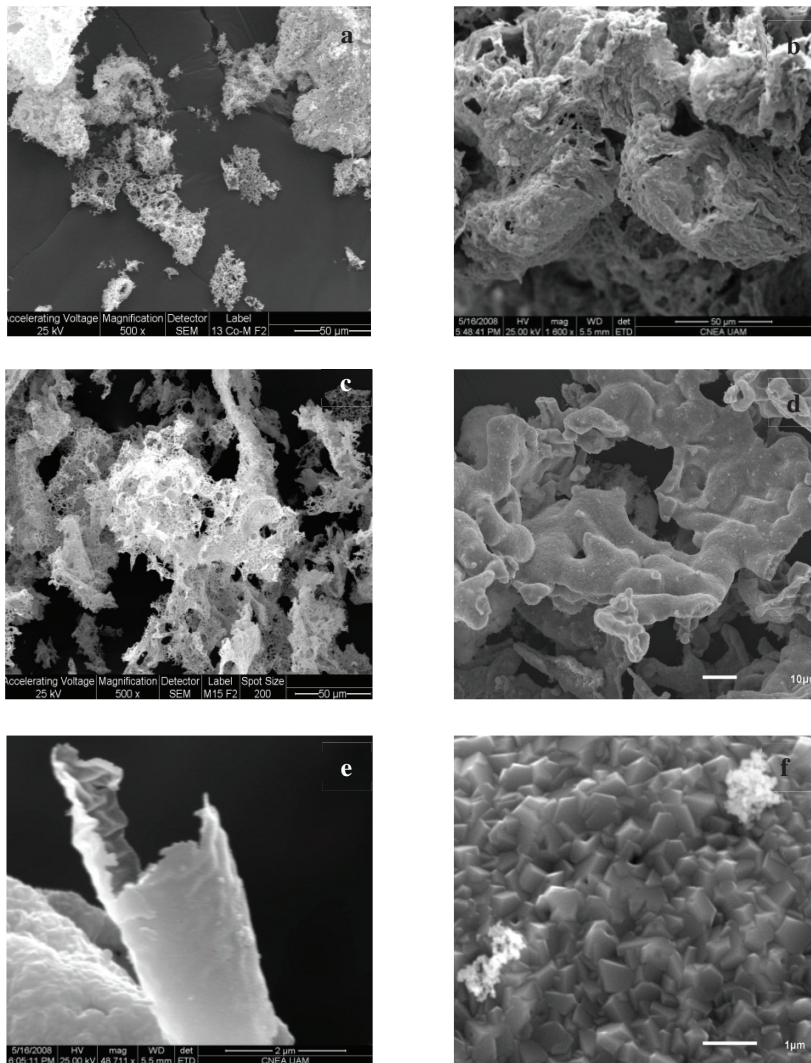


Fig. 2. SEM micrographs of (a)  $\text{Co}_3\text{O}_4\text{-S-Asp}$ ; (b)  $\text{Co}_3\text{O}_4\text{-NS-Asp}$ ; (c)  $\text{Co}_3\text{O}_4\text{-S-Tris}$ ; (d)  $\text{Co}_3\text{O}_4\text{-NS-Tris}$ ; (e)  $\text{Co}_3\text{O}_4\text{-NS-Asp}$ ; (f)  $\text{Co}_3\text{O}_4\text{-NS-Tris}$ .

Among the four powders, the  $\text{Co}_3\text{O}_4\text{-S-Asp}$  ones were selected for studying their optical properties, because the efficiency in their synthesis was the best, in terms of the relative mass of produced pigment. The aim of this characterization was to verify their optical properties before the production of solar paints. The resulting solar absorption was 86%. These results evidence their aptitude to be used in solar absorbent paints. Solar selective surfaces composed of copper or aluminum substrates painted with alkyd- $\text{Co}_3\text{O}_4$  paints presented lumps and rough finishes. Solar absorptance values on both surfaces were 93%. Likewise, in similar studies for selective surfaces composed by  $\text{Co}_3\text{O}_4$ -acrylic paints applied over aluminum foils the compared values were between 88-94% (Van Buskirk (1982)). For aluminum and copper surfaces, a high thermal emittance value of 90% was measured for its high thicknesses of 51 and 68  $\mu\text{m}$  respectively. So, low emittance values characteristics of metallic substrates seem to have little significant influence and, probably with a minor width thermal emittance values would drop.

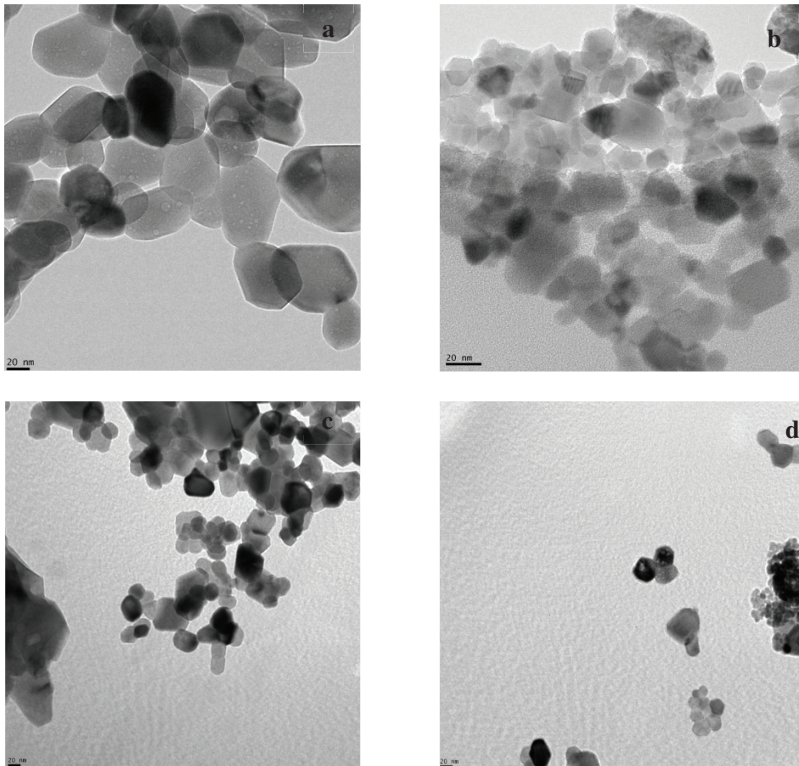


Fig. 3. TEM micrographs of (a)  $\text{Co}_3\text{O}_4\text{-S-Asp}$ ; (b)  $\text{Co}_3\text{O}_4\text{-NS-Asp}$ ; (c)  $\text{Co}_3\text{O}_4\text{-S-Tris}$ ; (d)  $\text{Co}_3\text{O}_4\text{-NS-Tris}$ .

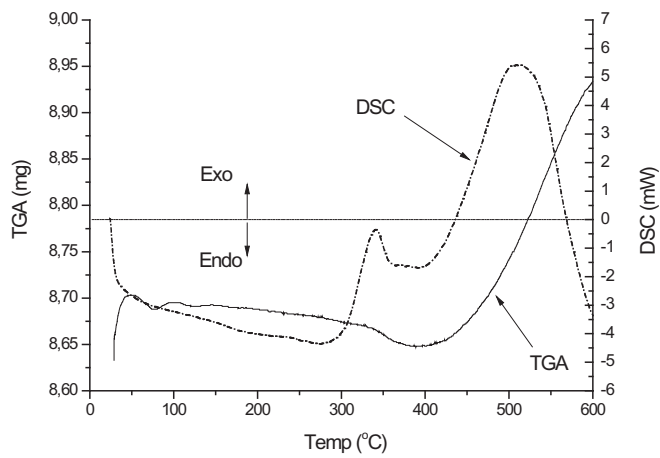


Fig. 4. Thermal analysis of the  $\text{Co}_3\text{O}_4\text{-NS-Asp}$  sample.

#### 4. Conclusion

In this work, two new gel-combustion processes for the synthesis of  $\text{Co}_3\text{O}_4$  nanopowders -with aspartic acid (Asp) or tri-hydroxi-methyl-aminomethane (Tris) as fuels- are presented. The first route is a conventional, stoichiometric process while the second is a non-stoichiometric, pH-controlled process. A spinel crystal structure of  $\text{Co}_3\text{O}_4$  was present in all obtained powders. A minimum value of the crystallite average size of 29 nm was observed for powders obtained by the “stoichiometric/Asp” combustion route; meanwhile, a maximum value of 41 nm was stated for powders obtained by the “non-stoichiometric/Asp” combustion process. In addition, the powders obtained by stoichiometric routes yielded lower average crystallite sizes than those obtained by non-stoichiometric processes, which was confirmed as a tendency in this material. By TEM, 50-100 nm-polyhedral particles were observed. Stoichiometric/Asp powders were selected to study optical properties. Their solar absorption value was 86%, evidencing their aptitude for solar absorbent paints, as compared with other related pigments described in scientific specialized bibliography. Two solar selective surfaces were obtained, both composed of  $\text{Co}_3\text{O}_4$  pigments and an alkyd resin applied over copper or aluminum substrates. In both cases, solar absorptance values were 93% but the thermal emittance value was over 90% as a consequence of the high width. So, low emittance values characteristics of metallic substrates seem to have little influence and, probably, with a minor width, thermal emittance values would drop.

#### Acknowledgements

The authors wish to express their thanks to Ing. Edgardo Soto and Lic. María E. Canafoglia, both from the CINDECA, for their valuable experimental measurements in adsorption-desorption of  $\text{N}_2$  and SEM, respectively. We also wish to thank the authorities of CONICET-Mendoza and of the UTN-FRM for their support in this research.

#### References

- Al-Tuwirqi, R., Al-Ghamdi, A. A., Aal, N. A., Umar A., Mahmoud, W. E., 2011. Facile synthesis and optical properties of  $\text{Co}_3\text{O}_4$  nanostructures by the microwave route. *Superlattices and Microstructures* 49, 416–421.
- Avila G., A., Barrera C, E., Huerta A., L., Muhl, S., 2004. Cobalt oxide films for solar selective surfaces, obtained by spray-pyrolysis. *Solar Energy Materials & Solar Cells*, 82, 269–278.
- Askarinejad, A., Morsali, A., 2009. Direct ultrasonic-assisted synthesis of sphere-like nanocrystals of spinel  $\text{Co}_3\text{O}_4$  and  $\text{Mn}_3\text{O}_4$ . *Ultrasonics sonochemistry* 16, 124.
- Barreca, D., Bekermann, D., Comini, E., Devi, A., Fischer, R. A., Gasparotto, A., Gavagnin, M., Maccato, C., Sada, C., Sberveglieri, G., Tondello, E., 2011. Plasma enhanced - CVD of undoped and fluorine-doped  $\text{Co}_3\text{O}_4$  nanosystems for novel gas sensors. *Sensors and Actuators B* 160, 79.
- Gui, Z., Zhu, J., Hu, Y., 2012. A simple preparative method for porous hollow-ware stacked cobalt oxides and their catalytic properties. *Materials Chemistry and Physics* 124, 243–247.
- Lascalea, G. E., 2004. Obtención y propiedades de polvos nanocristalinos y materiales cerámicos de grano submicrométrico basados en circonia. Tesis para optar al título de Doctor en Ciencia y Tecnología, Mención Materiales. Instituto Sabato/Universidad Nacional de San Martín, Buenos Aires, Argentina.
- Luisetto, I., Pepe, F., Bemporad, E., 2008. Preparation and characterization of nano cobalt oxide. *Journal of Nanoparticle Research* 10, 59.
- Ozkaya, T., Baykal, A., Toprak, M. S., Koseoğlu, Y., Durmuş, Z., 2009. Reflux synthesis of  $\text{Co}_3\text{O}_4$  nanoparticles and its magnetic characterization. *Journal of Magnetism and Magnetic Materials* 321, 2145.
- Pal, J., Chauhan, P., 2010. Study of physical properties of cobalt oxide ( $\text{Co}_3\text{O}_4$ ) nanocrystals. *Materials Characterization* 6, 575
- Tang, X., Li, J., Hao J., 2008. Synthesis and characterization of spinel  $\text{Co}_3\text{O}_4$  octahedra enclosed by the {1 1 1} facets”, *Materials Research Bulletin* 43, 2912-2918.
- Thangavelu, K., Parameswari, K., Kuppasamy, L., Haldorai, Y., 2011. A simple and facile method to synthesize  $\text{Co}_3\text{O}_4$  nanoparticles from metal benzoate dihydrazinate complex as a precursor. *Materials Letters* 65, 1482.
- Toniolo, J., Takimi, A., Bergmann, C. Nanostructured cobalt oxides ( $\text{Co}_3\text{O}_4$  and  $\text{CoO}$ ) and metallic Co powders synthesized by the solution combustion method. *Materials Research Bulletin* 45 (2010) 672.
- Trease, C. H., Hadavinia H., Barrington, P. E., 2013. Solar Selective Coatings: Industrial State-of-the-Art. *Recent Patents on Materials Science* 6, 1.
- Van Buskirk O. R., 1982. Solar selective surfaces; US 4310596. Jan, 12.



- Venkateswara, Rao, K., Sunandana, C., 2008. Co<sub>3</sub>O<sub>4</sub> nanoparticles by chemical combustion: Effect of fuel to oxidizer ratio on structure, microstructure and EPR. *Solid State Communications* 148, 32.
- Vince, J., Šurca Vuk, A., Opara Krašovec, U., Orel, B., Köhl, M., Heck, M., 2003. Solar absorber coatings based on CoCuMnO<sub>x</sub> spinels prepared via the sol–gel process: structural and optical properties. *Solar Energy Materials & Solar Cells* 79, 313.
- Yang, H., Yuehua, H., Xiangchao, Z., Guanzhou, Q., 2004. Mechanochemical synthesis of cobalt oxide nanoparticles. *Materials Letters* 58, 387.
- Yang, L., Guan, W., Bai, B., Xu, Q., and Xiang, Y., 2010. Synthesis of yeast-assisted Co<sub>3</sub>O<sub>4</sub> hollow microspheres - A novel biotemplating technique. *Journal of Alloys and Compounds* 504, L10.